HYDROLYSIS AND NEUTRALIZATION PROCESSES OF HYDROXY SODALITE

B. Kutus*, M. Asher, I. Kovács, P. Sipos

Department of Molecular and Analytical Chemistry, University of Szeged, 7–8 Dóm tér, H–6720 Szeged, Hungary

**Corresponding author: kutusb@chem.u-szeged.hu*

ABSTRACT

Being one of the reactive phases present in bauxite residues, the dissolution of hydroxy sodalite or HXS, $Na_8[AlSiO_4]_6(OH)_2 \cdot mH_2O$, gives rise to a strongly alkaline environment in residue slurries. To effectively decrease the environmental hazards of bauxite residue via acid neutralization, it is pivotal to understand the neutralization mechanism as well as dissolution processes of HXS. To this end, we synthesized HXS and studied its hydrolysis as well as neutralization reactions using hydrochloric acid. We find that increasing the solid:liquid mass ratio results in a significant increase in the pH and dissolved metal concentrations, evidencing the incongruent dissolution of HXS. The secondary phases forming during this process are two types of hydrosodalite (HS1 and HS2), being dominant below pH ~ 10. Upon addition of HCl, the pH readily drops to ~7, suggesting rapid neutralization kinetics. Concomitantly, HXS transforms to HS1, giving rise to a slow increase in pH, before reaching a steady-state value of ~10.3.

1. INTRODUCTION

Red mud or bauxite residue (BxR) is the main by-product of the Bayer process [1–3]. In general, 0.5–2 tons of residue are generated per ton of alumina [4], which yielded more than 140 million tons of alumina in 2022 [5]. BxR has potential applications in the building and wastewater industries, as well as in revegetation [6]. However, a wide-scale utilization of BxR requires to reduce its high alkalinity to below pH = 9 [7] via neutralization [1,3,8].

Prior to discharge, acidic pre-treatment can readily decrease solution alkalinity. Conversely, a significant fraction of basicity stems from reactive solid phases forming via the Bayer process [1,3]. This so-called solid alkalinity gives rise to a buffering capacity of BxR in the pH range of 6–10, as well as a rebounding of pH after rapid neutralization [1,3,8]. In this respect, one of the most important reactive phases is hydroxy sodalite or HXS ($Na_8[SiAlO_4]_6(OH)_2 \cdot xH_2O$, x = 2–6) [9,10]. HXS is formed in the pre-desilication step at ~100 °C via the dissolution of kaolinite, $Al_2Si_2O_5(OH)_4$, present in bauxites [1,3,6,9].

To enhance the efficiency of BxR neutralization, understanding the mechanistic, kinetic, and thermodynamic aspects of dissolution and neutralization processes of HXS is indispensable. In this regard, the nature of the hydrolytic processes of sodalite has remained elusive, with only a very few quantitative studies published [11,12]. The goal of our work is to study the temporal evolution of the solubility and neutralization of HXS, as well as to identify possible secondary phases forming.

2. EXPERIMENTAL

2.1 Synthesis and characterization of HXS

Based on a procedure reported earlier [13], we prepared HXS by dissolving “eckalite1” kaolinite (Imerys Mineral, Australia) in concentrated, carbonate-free NaOH (18.6 M) / $NaAl(OH)_4$ (3.9 M) or neat NaOH (18.6 M) solutions at ~95 °C under continuous stirring for 1 or 2 days. The use of $NaAl(OH)_4$ or the reaction time did not impact neither the structure nor the composition of the solids. The purity of the HXS was checked by its X-ray powder diffractogram and matched very well with that of a literature reference (PDF no. 11–0401) [14]. In addition, all characteristic Al-O-Si framework vibrations were identified in the infrared spectra of HXS [15,16]. The ideal Na:Al:Si elemental ratio of 8:6:6 was confirmed with inductively coupled plasma mass spectrometry (ICP-MS). Thermogravimetric

(TG-MS) analysis showed that HXS was essentially free of carbonate, while total carbon (TC) detection showed the presence of CO_3^{2-} (being as minor anion compared to OH^-). Combining the three methods, the composition was found to be $Na_8[SiAlO_4]_6(OH)_{1.6}(CO_3)_{0.2}{\cdot}2.8H_2O$.

2.2 Dissolution and neutralization experiments

In the first set of experiments, the solubility was studied by varying the mass concentration of HXS from 0.01 to 100 g L^{-1}. After the addition of solid, samples were stirred continuously, and the temporal evolution of pH was monitored by regular readings. As a result, 20–30 days were found to be sufficient to attain equilibrium. Nevertheless, as this type of experiment makes it difficult to avoid the dissolution of aerial CO_2, another experiment was carried out from a third lot of HXS, where the pH of suspensions was only measured once (after 30–33 days of contact time). The types of solubility experiments are listed in Table 1. After the equilibration period, all samples were filtered, the supernatants were analysed for $[Na]_T$, $[Al]_T$, and $[Si]_T$ via ICP-MS. ($[X]_T$ refers to the total dissolved molar concentration of Na^+, silicate or aluminate ions.) In addition, filter cakes were dried under infrared lamp and their powder X-ray diffractograms were measured.

Table 1. Types of dissolution experiments.

Series of experiment	Reaction time / day	pH readings before filtration
#1	20	regularly
#2	30	regularly
#3	30	once

In the second series of experiments, a solution series with c_{HXS} = 10 g L^{-1} was prepared, and HCl, equivalent to the amount of OH^- and CO_3^{2-} ions in HXS, was added to the suspensions. Following acid addition, solution pH was measured after different reaction times (up to 14 days), right before the filtration step. Supernatants and solid phases were analysed again with ICP-MS and XRD methods.

All samples were made from deionised water and measurements were carried out at room temperature.

2.3 Methods

The pH of the suspensions were measured by a SevenEasy pH meter (Mettler Toledo), using a combined glass electrode (Sentix H by WTW). In each case, the electrode was calibrated with commercial buffers in the pH range of 1.68–13.0. The elemental composition (Na, Al, Si) of the supernatants were quantified by an Agilent 7900 ICP-MS spectrometer. Before measurement, all samples were diluted to an appropriate degree, and cc. HNO_3 (Aristar®, VWR Chemicals) was added to the solutions up to 2 wt%. Both calibration and samples series contained 0.1 ppm internal standard (Sc and Y, Aristar®, VWR Chemicals).

The X-ray diffractogram of the solids was measured using a Rigaku Miniflex II instrument, with a CuKα or CoKα radiation source (1.5418 or 1.7902 Å), 2–4° min^{-1} scanning rate and 0.02° step width. For dilute suspensions, the most informative 55–67° 2θ region was noisy; thus, noise was filtered out numerically using the Savitzky-Golay function. For as-prepared sodalites, vibration spectra were collected with a Jasco 4700 FT-IR spectrometer with an optical resolution of 4 cm^{-1} in attenuated total reflection mode, applying a ZnSe crystal and deuterated triglycine sulphate detector. The water content was determined using a TA Instruments Discovery TGA analyzer coupled to a mass spectrometer (MS, Hiden Analytical, HPR-20 EGA) under air at 10°C min^{-1} heating rate.

3. RESULTS AND DISCUSSION

3.1 Dissolution of HXS – analysis of the aqueous phase

In the first experimental series, we studied the time evolution of pH by varying the mass concentration of HXS (0.01–100 g L^{-1}). The measured values are shown in Figure 1. It is seen that the pH increases sharply in the first 1–2 days, due to the release of OH^- ions. Based on the composition determined via ICP TG, and TC, this can be elucidated by the reaction:

$$Na_8[SiAlO_4]_6(OH)_{1.6}(CO_3)_{0.2}{\cdot}2.8H_2O + 21.2H_2O \rightleftharpoons 8Na^+ + 7.6OH^- + 0.2CO_3^{2-} + 6H_4SiO_4 + 6Al(OH)_3 \quad (1)$$

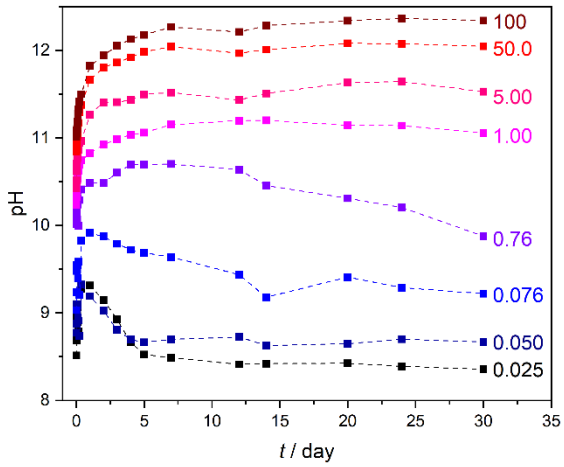

Figure 1. Change in solution pH as a function of reaction time during the dissolution of hydroxy sodalite, HXS. The initial mass concentrations in g L^{-1} for selected datasets are also shown. Dashed lines serve as a guide to the eye.

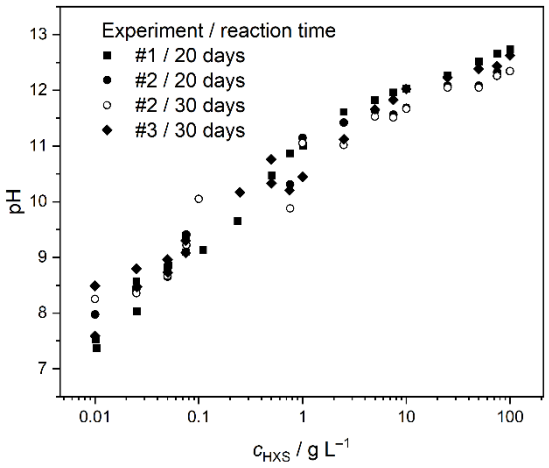

Figure 2. Dependence of solution pH in equilibrated suspensions of hydroxy sodalite, HXS, as a function of its initial mass concentration. The suspensions were filtered after 20 or 30 days. For #2, data after 20 days are also shown.

Expectedly, concentrated suspensions (c_{HXS} > 1 g L^{-1}) show the pH to continuously increase over time. It is however unclear whether the sharp maxima appearing for dilute systems (c_{HXS} < 1 g L^{-1}), followed by a decrease in pH, are inherent to the dissolution of HXS or it is due to carbonation. Also, frequent measuring of pH might cause the solid to stick to the surface of the electrode, resulting in continuous removal of the solid, which can in turn affect the pH. Nevertheless, it is seen that 20–30 days are sufficient to reach dissolution equilibrium.

To obtain a statistically meaningful variation of pH as a function of c_{HXS}, and to assess the effect of incidental carbonation, a third series were prepared, and the pH was measured only before filtration. The results for all the three series are plotted in Figure 2. It demonstrates that independent of the applied reaction time, and the frequency of pH readings, all data fit into a characteristic trend. That is, increasing the mass of solid, the pH increases markedly from ~8 to ~12.5. (Expectedly, the data are more scattered for dilute mixtures.) The dependence of pH on solid:liquid ratio indicates that HXS dissolves incongruently, i.e. the elemental ratios in the aqueous and in the solid phase are not equal. Previously, the same effect has been observed for hydroxyapatite, too [17].

Solution-phase metal concentrations as measured by ICP-MS are shown in Figure 3. It is seen that $[Na]_T$ concentrations significantly exceed the values of $[Al]_T$ and $[Si]_T$, the difference being more than one order of magnitude above pH ~ 12. Since the ideal Na:Si and Na:Al ratio should be 1.33 [10], our findings provide sound evidence for the incongruent dissolution of HXS.

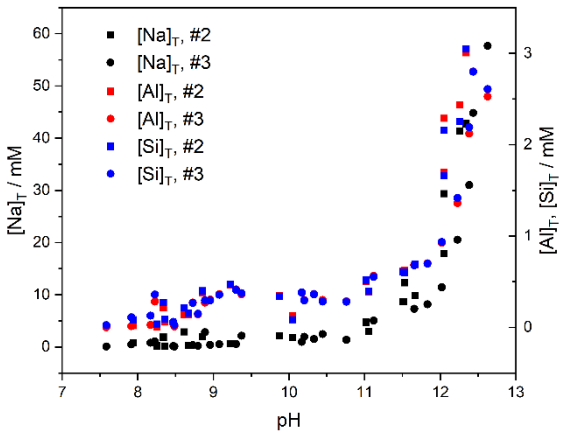

Figure 3. Dependence of total concentrations of dissolved Na, Al, and Si in equilibrated suspensions of hydroxy sodalite, HXS, as a function of pH (experiments #2 and #3).

This process can be explained by the formation of hydrosodalite, HS, which has the same Al-O-Si framework as HXS, but is absent of cage OH^- ions [10,15].

$$Na_8[SiAlO_4]_6(OH)_{1.6}(CO_3)_{0.2}\cdot 2.8H_2O + 5.2H_2O \rightleftharpoons Na_6[SiAlO_4]_6\cdot 8H_2O + 1.6Na^+ + 1.6OH^- + 0.2CO_3^{2-} \quad (2)$$

This reaction yields an excess of Na^+ ions as compared to aluminate and silicate species. On the other hand, the presence of the latter two indicates the dissolution of HXS/HS framework to take place as well (Eq. 1). Overall, the mechanism of the dissolution of HXS can be elucidated as a sequential process. That is, the first step is always the formation of a HS crystal (Eq. 2), which might be followed by further disintegration of the structure (Eq. 1). Based on the abundance of Na^+ ions in these systems, the first step is thermodynamically more favourable.

Interestingly, the concentrations of all the three ions increase markedly above pH ~ 11. Most probably, this is associated with the enhanced formation of $Al(OH)_4^-$ and $H_3SiO_4^-$ aqueous species [1], rendering the framework dissolution to be markedly enhanced in the strongly alkaline region:

$$Na_8[SiAlO_4]_6(OH)_{1.6}(CO_3)_{0.2}\cdot 2.8H_2O + 4.4OH^- + 15.2H_2O \rightleftharpoons 8Na^+ + 0.2CO_3^{2-} + 6H_3SiO_4^- + 6Al(OH)_4^- \quad (3)$$

It is worth noting that the Si:Al molar ratio is some 5–10 times higher than 1:1 below pH~9, suggesting the presence of solid $Al(OH)_3$. On the other hand, the Si:Al ratio is 1:1 above this pH, as expected from Eqs. (1) and (3).

3.2 Dissolution of HXS – analysis of the solid phase

The X-ray powder diffractograms (exp. Series #3) are depicted in Figure 4. Strikingly, we find two equilibrium solid phases with respect to dilute suspensions (c_{HXS} = 0.5–1 g L^{-1}). Based on pioneering studies on HXS and HS, these two phases can be identified as HS1 and HS2, with formulas of $Na_{6.4}[SiAlO_4]_6\cdot 0.2CO_3\cdot 6H_2O$ and $Na_6[SiAlO_4]_6\cdot 8H_2O$, respectively [10,15]. The formation of these hydrosodalites indeed explains the incongruent dissolution of HXS. Moreover, the presence of CO_3^{2-} ions in HS_1 can be attributed to the carbonate content found already in the as-prepared HXS. The existence of the "ideal" hydrosodalite, HS2, suggests the following equilibrium:

$$Na_6[SiAlO_4]_6\cdot 8H_2O\cdot 8H_2O + 0.2CO_3^{2-} \rightleftharpoons Na_{6.4}[SiAlO_4]_6(CO_3)_{0.2}\cdot 6H_2O + 2H_2O \quad (4)$$

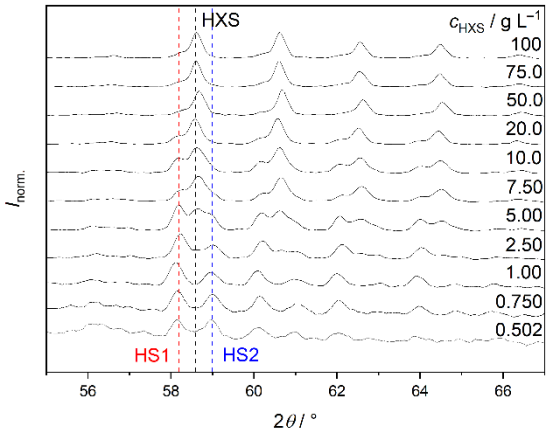

Figure 4. Traces of X-ray powder diffractograms of solids obtained from equilibrated suspensions of hydroxy sodalite, HXS (experiment #3). Horizontal dashed lines indicate the positions of HXS and two hydrosodalite, HS, phases. The data were smoothed using the Savitzy-Golay filter and were normalized such that the highest intensity is unity.

The appearance of HS2 at low c_{HXS} and pH might arise from the protonation of CO_3^{2-} (i.e. the formation of HCO_3^-), which decreases the concentration of dissolved carbonate and thus favours its release from HS1.

In conclusion, HXS is absent in dilute, equilibrated suspensions, whereas it is the dominant solid phase in concentrated mixtures. Nevertheless, HS1 is still present as minor phase even at c_{HXS} = 100 g L^{-1}, in line with the excess Na^+ ions found in concentrated suspensions.

3.3 Neutralization of HXS – analysis of the aqueous phase

In general, invariant of the relative fraction of OH^- and CO_3^{2-} ions in the sodalite cage, neutralization of the solid (with a target pH of 7–8) requires 2 equivalents of H^+ ions. Hence, to assess the progress of neutralization, we added 2 equiv. of HCl to suspensions of 10 g L^{-1}. The pH values measured after different reaction times, where t = 0 corresponds to the addition of acid, are shown in Figure 5.

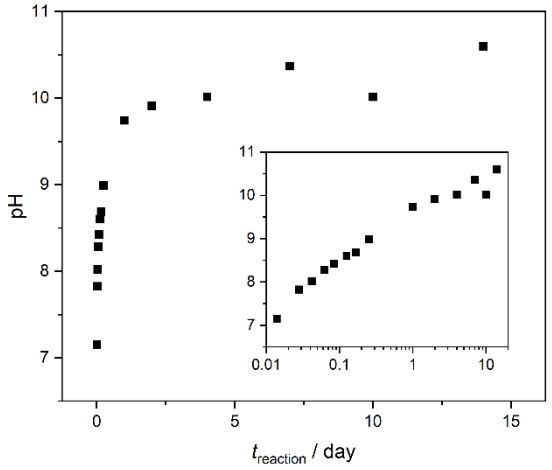

Figure 5. Change in solution pH as a function of reaction time during the neutralization of hydroxy sodalite, HXS. 2 equivalents of 1 M HCl was added to each suspension with c_{HXS} = 10 g L^{-1} at the onset of reactions. The inset shows the same variation on the logarithmic timescale.

We find the pH to be ~7 already after 20 minutes, which demonstrates, similarly to acid-base reactions in an aqueous medium, that the neutralization of cage-like OH^- and CO_3^{2-} ions are virtually instantaneous. Conversely, the pH continues to increase over 2 weeks, attaining a steady-state value of ~10.3. This slow but gradual rise in pH has been referred to as the rebounding of pH or "pH bounce-back", which arises from the slow dissolution of the solid in contact with its aqueous phase.

Concomitantly, the concentration of Na^+ reaches almost its maximum value after 20 minutes, then starts to slowly rise by 8–10% over 2 weeks. At the same time, the presence of Si and Al already at the beginning of reaction indicates a partial disintegration of the sodalite framework, too. Surprisingly, the concentrations of the two species vary in the opposite way. Consequently, excess Si is being incorporated into a forming phase, whereas the increase in Al signals the transformation of $Al(OH)_3$ to a more soluble sodalite phase. Furthermore, similarly to the dissolution of HXS, the Si:Al ratio becomes 1:1 as the reaction progresses.

3.3 Neutralization of HXS – analysis of the solid phase

The powder diffractograms of the solids collected from the samples at given reaction times are seen in Figure 6. Compared to the reference solid, i.e. as-prepared HXS, the solid forming readily upon acid addition is HS1. This finding is in excellent agreement with this solid being equilibrium with HXS at 10 g L^{-1} during its dissolution (see Figure 4). Furthermore, it suggests the CO_3^{2-} to be retained in the sodalite cage, contrary to OH^-. In conclusion, the rapid neutralization of HXS can be summarized as follows:

$$Na_8[SiAlO_4]_6(OH)_{1.6}(CO_3)_{0.2}\cdot 2.8H_2O + 1.6H^+ + 1.6H_2O \rightleftharpoons Na_{6.4}[SiAlO_4]_6\cdot(CO_3)_{0.2}\cdot 6H_2O + 1.6Na^+ \quad (5)$$

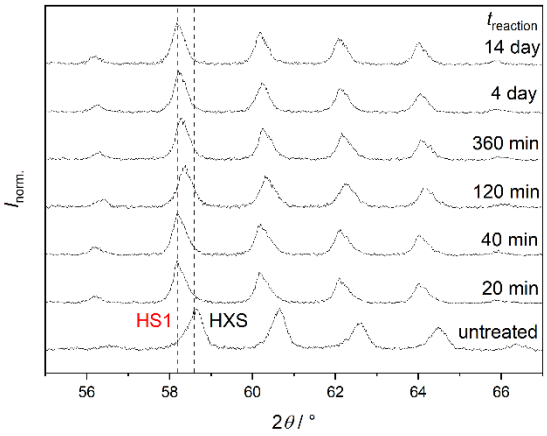

Figure 6. Traces of X-ray powder diffractograms of solids obtained from 10 g L^{-1} suspensions of hydroxy sodalite, HXS, at different reaction times following the addition of 2 equivalents of 1 M HCl. Horizontal dashed lines indicate the positions of HXS and a hydrosodalite, HS1. All diffractograms were normalized such that the highest intensity is unity.

Following this reaction, dissolution reactions of both $Al(OH)_3$ (forming due to framework dissolution) and HS1 (similar to the one in Eq. 1) give rise to the gradual increase or rebounding of pH.

4. CONCLUSION

In this work, we studied the dissolution and neutralization reactions of HXS, which often constitutes a major reactive phase in BxR slurries.

We found from the strong dependence of pH and solubility on the solid:liquid mass ratio that HXS dissolves incongruently. The thus forming secondary phases comprise $Al(OH)_3$, and two hydrosodalite phases, HS1 and HS2, with HS1 containing carbonate ion in its Al-O-Si

framework. Upon increasing the amount of solid, the pH increases steadily up to ~12.5, which in turn promotes the dissolution of HXS via the formation of $H_3SiO_4^-$ and $Al(OH)_4^-$ ions.

Upon addition of HCl, structure OH^- ions of HXS react rapidly, yielding an initial pH of ~7. Simultaneously, HXS transforms to HS1, and the slow dissolution of the latter results in a slow increase in pH, a phenomenon that has been coined “pH bounce-back” in literature.

In conclusion, not only HXS but also HS must be taken into account for the neutralization of bauxite residue.

5. REFERENCES

[1] Gräfe, M., Power, G., Klauber, C. 2011. Bauxite residue issues: III. Alkalinity and associated chemistry. Hydromet. 108, 60–79. https://doi.org/10.1016/j.hydromet.2011.02.004

[2] Vogrin, J., Hodge, H., Santini, T., Peng, H., Vaughan, J. 2019. Quantitative X-Ray Diffraction Study into Bauxite Residue Mineralogical Phases, Chesonis, C. (Ed.), Light Metals 2019, Springer, Cham, Switzerland, pp. 93–99. https://doi.org/10.1007/978-3-030-05864-7_13

[3] Kirwan, L. J., Hartshorn, A., McMonagle, J. B., Fleming, L., Funnell, D. 2013. Chemistry of bauxite residue neutralisation and aspects to implementation. Int. J. Miner. Process. 119, 40–50. https://doi.org/10.1016/j.minpro.2013.01.001

[4] Kong, X., Li, M., Xue, S., Hartley, W., Chen, C., Wu, C., Li, X., Li, Y., 2017. Natural evolution of alkaline characteristics in bauxite residue. J. Hazard. Mater. 324B, 382–390. https://doi.org/10.1016/j.jclepro.2016.12.125

[5] International Aluminium Institute. Alumina Production. https://international-aluminium.org/statistics/alumina-production/ (accessed 26 January 2024)

[6] Evans, K., 2016. The history, challenges, and new developments in the management and use of bauxite residue. J. Sustain. Metall. 2, 316–331. https://doi.org/10.1007/s40831-016-0060-x

[7] Gräfe, M., Klauber, C., 2011. Bauxite residue issues: IV. Old obstacles and new pathways for in situ residue remediation, 2011. Hydromet. 108 46–59. https://doi.org/10.1016/j.hydromet.2011.02.005

[8] Khaitan, S., Dzombak, D. A., Lowry, G. V., 2009. Chemistry of acid neutralization capacity of bauxite residue. Environ. Eng. Sci. 26, 873–881. https://doi.org./10.1089/ees.2007.0228

[9] Whittington, B. I., Fletcher, B. L., Talbot, C., 1998. The effect of reaction conditions on the composition of desilication product (DSP) formed under simulated Bayer conditions. Hydromet. 49, 1–22. https://doi.org/10.1016/S0304-86X(98)00021-8

[10] Engelhardt, G., Felsche, J., Sieger, P., 1992. The hydrosodalite system $Na_{6+x}[SiAlO_4]_6(OH)_x{\cdot}nH_2O$. Formation, phase composition, and de- and rehydration studied by ‘H, ^{23}Na, and ^{29}Si MAS-NMR spectroscopy in tandem with thermal analysis, X-ray diffraction, and IR spectroscopy. J. Am. Chem. Soc. 114, 1173–1182. https://doi.org/10.1021/ja00030a008

[11] Xiong, 2016. Solubility constants of hydroxyl sodalite at elevated temperatures evaluated from hydrothermal experiments: Applications to nuclear waste isolation. J., Appl. Geochem. 74, 138–143. https://dx.doi.org/10.1016/j.apgeochem.2016.09.009

[12] Zheng, L., Li, Z., 2012. Solubility and modeling of sodium aluminosilicate in $NaOH{-}NaAl(OH)_4$ solutions and its application to desilication. Ind. Eng. Chem. Res. 51, 15193–15206. https://dx.doi.org/10.1021/ie301590r

[13] Kása, E., Szabados, M., Baán, K., Kónya, Z., Kukovecz, Á., Kutus, B., Pálinkó, I., Sipos, P., 2012. The dissolution kinetics of raw and mechanochemically treated kaolinites in industrial spent liquor – The effect of the physico-chemical properties of the solids. Appl. Clay Sci. 203, 105994. https://doi.org/10.1016/j.clay.2021.105994

[14] Gates-Rector, S., Blanton, T., 2019. The powder diffraction file: a quality materials characterization database. Powder Diffract. 34, 352–360. https://doi.org/10.1017/S0885715619000812

[15] Hermeler, G., Buhl, J-Ch., Hoffmann, W., 1991. The influence of carbonate on the synthesis of an intermediate phase between sodalite and cancrinite. Catal. Today 8, 415–426. https://doi.org/10.1016/0920-5861(91)87020-N

[16] Deng, Y., Harsh, J. B., Flury, M., Young, J. S., Boyle, J. S., 2006. Mineral formation during simulated leaks of Hanford waste tanks. Appl. Geochem. 21, 1392–1409. https://doi.org/10.1016/j.apgeochem.2006.05.002

[17] Kaufman, H. W., Kleinberg. I., Studies on the incongruent solubility of hydroxyapatite, 1979. Calcif. Tiss. Intl. 27, 143–151. https://doi.org/10.1007/BF02441177.